

**PCCP****Amplified Spontaneous Emission in Phenylethylammonium Methylammonium Lead Iodide Quasi-2D Perovskites**

Journal:	<i>Physical Chemistry Chemical Physics</i>
Manuscript ID	CP-ART-04-2018-002133.R1
Article Type:	Paper
Date Submitted by the Author:	15-May-2018
Complete List of Authors:	Leyden, Matthew R.; Kyushu University, Center for Organic Photonics and Electronics Research (OPERA) matsushima, toshinori; Kyushu Univ., OPERA Qin, Chuanjiang; Kyushu Univ., OPERA Ruan, Shibin; Kyushu University, Center for Organic Photonics and Electronics Research (OPERA) Ye, Hao; Kyushu University, Center for Organic Photonics and Electronics Research (OPERA) Adachi, Chihaya; Kyushu University, Center for Organic Photonics and Electronics Research (OPERA)

SCHOLARONE™
Manuscripts



Physical Chemistry Chemical Physics

ARTICLE

Amplified Spontaneous Emission in Phenylethylammonium Methylammonium Lead Iodide Quasi-2D Perovskites

Matthew R. Leyden^{a,b}, Toshinori Matsushima^{a,b,c}, Chuanjiang Qin^{a,b}, Shibin Ruan^{a,b}, Hao Ye^{a,b}, Chihaya Adachi^{a,b,c*}

Received 00th January 20xx,
Accepted 00th January 20xx

DOI: 10.1039/x0xx00000x

www.rsc.org/

Organo-metal-halide perovskites are a promising set of materials for optoelectronic applications such as solar cells, light emitting diodes and lasers. Perovskite thin films have demonstrated amplified spontaneous emission thresholds as low as $1.6 \mu\text{J}/\text{cm}^2$ and lasing thresholds as low as $0.2 \mu\text{J}/\text{cm}^2$. Recently the performance of perovskite light emitting diodes has rapidly risen due to the formation of quasi 2D films using bulky ligands such as phenylethylammonium. Despite the high photoluminescent yield and external quantum efficiency of quasi 2D perovskites, few reports exist on amplified spontaneous emission. We show within this report that the threshold for amplified spontaneous emission of quasi 2D perovskite films increases with the concentration of phenylethylammonium. We attribute this increasing threshold to a charge transfer state at the PEA interface that competes for excitons with the ASE process. Additionally, the comparatively slow inter-grain charge transfer process cannot significantly contribute to the fast radiative recombination in amplified spontaneous emission. These results suggest that relatively low order PEA based perovskite films that are suitable for LED applications are not well suited for lasing applications. However high order films were able to maintain their low threshold values and may still benefit from improved stability.

INTRODUCTION

Recently many reports of organo-metal-halide perovskite materials such as methylammonium lead iodide (MAPbI_3) have shown promising performance for light emitting applications.¹ Lasing applications seem particularly promising as perovskite materials have shown amplified spontaneous emission (ASE) thresholds as low as $1.6 \mu\text{J}/\text{cm}^2$,² and lasing thresholds as low as $0.2 \mu\text{J}/\text{cm}^2$ using a Fabry-Perot cavity.³ Lasing cavities have been made using a variety of different structures such as distributed feedback gratings,⁴ and single crystal resonators.⁵ These low thresholds are now becoming competitive with other high performance organic lasing materials ($\sim 0.3 \mu\text{J}/\text{cm}^2$).⁶ Most of these reports have used lead based perovskite, but tin has also demonstrated ASE, but with a notably higher threshold.⁷

2D perovskites use a bulky ligand such as phenylethylammonium (PEA) to sandwich metal halide octahedra to form a 2D structure ($n=1$, Fig. 1). Specifically the material $(\text{PEA})_2\text{PbI}_4$ has a relatively high exciton binding energy and was used in light emitting diodes as early as 1994.⁸ Additionally Kondo et al. reported bi-excitonic lasing at low temperatures in 1998.⁹ However a more recent report from Chong et al. claimed it to be difficult to use for lasing

applications,¹⁰ as the authors were unable to demonstrate ASE even at low temperature and high pump fluence. They claimed that the previous report showed band narrowing but not ASE, and attributed the inability to form ASE with the formation of bound excitons and Bi-excitons that competed with ASE pathways. Based on data fitting from experiments they predicted a high ASE threshold of $1.4 \text{ mJ}/\text{cm}^2$, which was well beyond the threshold required to damage the film.

Quasi 2D perovskites are a hybrid of the two extremes between 3D and 2D perovskites. These perovskites can be defined by the order n , where n defines the number of metal halide octahedral sandwiched in between bulky ligands, specifically $(\text{PEA})_2 \text{MA}_{(n-1)} \text{Pb}_n \text{I}_{(3n+1)}$ (Fig. 1a). Quasi 2D perovskites have a balance between the better charge transport behavior of 3D perovskites, and the better radiative recombination at lower excitation energies of 2D perovskite.¹¹⁻¹³ Despite having a distribution of material with varying band gaps, quasi 2D perovskites keep a relatively narrow emission spectrum due to an inter-grain charge transfer process.¹¹ An approximate timescale for relevant light emitting processes is presented in Fig. 1b. In the charge transfer process, excited carriers within a large bandgap grain are funneled to a neighbor grain with a smaller bandgap, where they will radiatively combine. From transient absorption spectroscopy, this inter-grain charge transfer process appears to require hundreds of picoseconds to nanoseconds to complete.¹¹ Because of these advantageous properties, quasi 2D perovskites have recently demonstrated high performance light emitting diodes with up to 11.7% external quantum efficiency.¹³ Given the high performance of these LEDs and the low lasing thresholds of

^a Center for Organic Photonics and Electronics Research (OPERA), Kyushu University, 744 Motoooka, Nishi, Fukuoka 819-0395, Japan

^b Japan Science and Technology Agency (JST), ERATO, Adachi Molecular Exciton Engineering Project, 744 Motoooka, Nishi, Fukuoka 819-0395, Japan

^c International Institute for Carbon Neutral Energy Research (WPI-I2CNER), Kyushu University, 744 Motoooka, Nishi, Fukuoka 819-0395, Japan

*Corresponding Author adachi@cstf.kyushu-u.ac.jp

Electronic Supplementary Information (ESI) available:

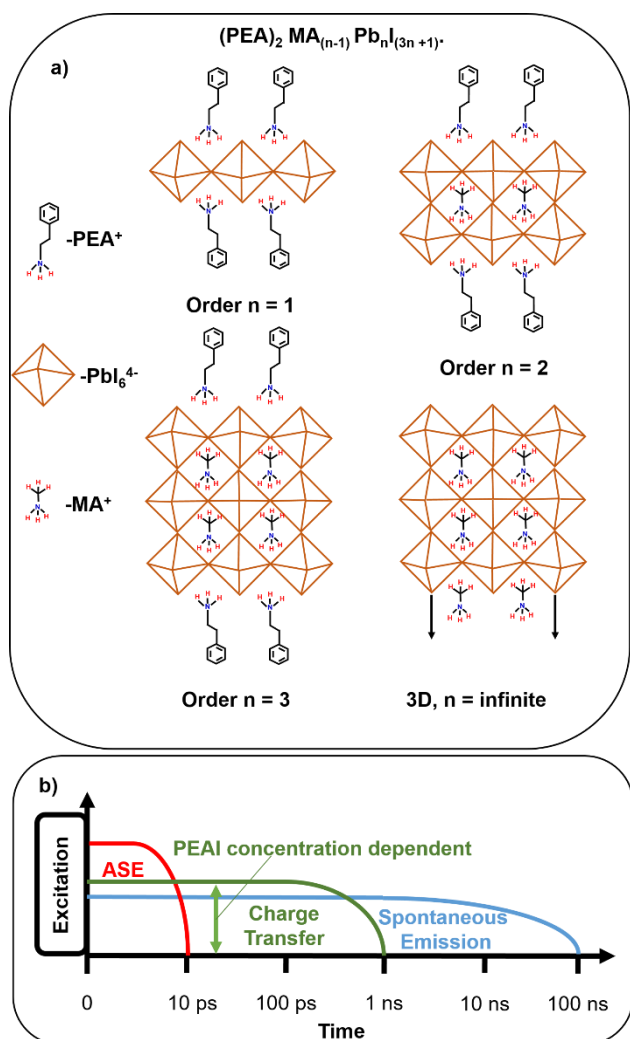


Figure 1. Diagram of quasi 2D perovskites. Order 1, also known as 2D perovskite, is a lead iodide octahedra sandwiched between two PEA cations forming a sheet. Orders 2 and above incorporate MA cations in the central structure. 3D perovskite has repeating units of lead iodide and MA cation, and no PEA cation. b) Approximate timeline of the excitation and emission processes in quasi 2D perovskite.

3D perovskites, quasi 2D perovskite may seem as promising candidates for electrically driven lasers. One may expect that lasing performance should exist between the two extremes reported for the 3D (MAPbI_3) $6 \mu\text{J}/\text{cm}^2$,² and the 2D structured ($(\text{PEA})_2\text{PbI}_4$) $1.4 \text{ mJ}/\text{cm}^2$.

Recent reports have shown that the cation octylammonium was used as a morphology regulator for MAPbBr_3 and was able to demonstrate ASE thresholds down to $\sim 18 \mu\text{J}/\text{cm}^2$.¹⁴ Another recent paper using solutions with low average order formamidinium (FA) / naphthylmethylammonium (NMA) based mixed halide perovskite found a threshold down to $\sim 19 \mu\text{J}/\text{cm}^2$ at $\sim 800 \text{ nm}$ wavelengths.¹⁵ In this referenced work they used thick films (600 nm) to demonstrate ASE and found a trend of increasing threshold with increasing dimensionality. This is interesting as it is opposite to the observations presented in our work. Differences can possibly be explained by faster charge transfer in the NMA system or a differing gain mechanism originating from a thicker film. Alternatively lower order material may act as a morphology regulator for the high order emitter similar to reference 14.

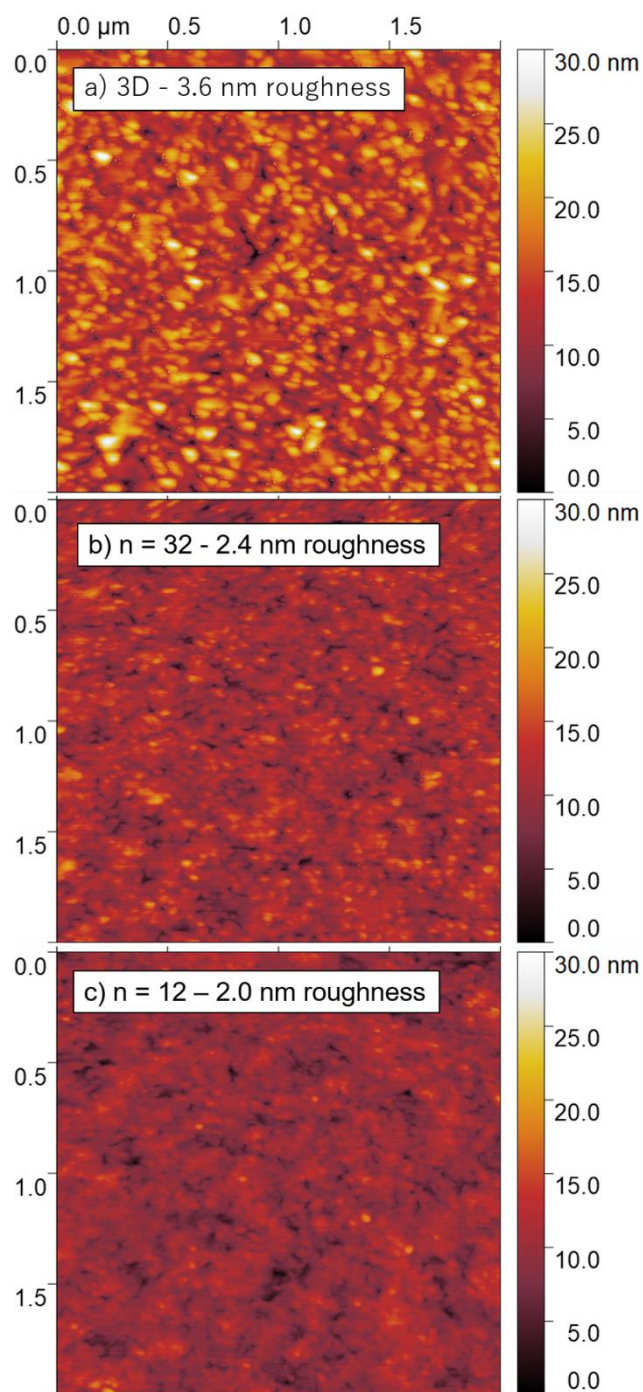
EXPERIMENTAL

Amplified Spontaneous Emission measurement. During ASE measurements films were pumped with a nitrogen laser (337 nm, 10 Hz, 0.8 nanosecond, Usho Optical Systems, KEN-2020). The excitation spot size was measured to be $\sim 0.01 \text{ cm}^2$ ($5.87 \times 1.69 \text{ mm}$, Fig. S1). Spectra were measured from the edge emission of a cleaved film. The light was passed through a long pass filter to remove the excitation light and then was focused with a convergent lens onto a fiber optic cable of a photonic multichannel analyzer (Hamamatsu C10027).

Perovskite film fabrication. Perovskite solutions were prepared in solutions of dimethylformamide using methylammonium iodide, phenylethylammonium iodide, and lead iodide. Methylammonium iodide and phenylethylammonium iodide were prepared by mixing methylamine or phenylethylamine with an equal molar amount of hydroiodic acid. The resulting powders were filtered, washed with diethyl ether, and then recrystallized in ethanol. Lead iodide was purchased from Tokyo Chemical Industry (TCI). The concentration of methylammonium iodide was at a 20% excess of being stoichiometric for a given order of perovskite. Specific concentrations are provided in Table S1. Perovskite films were prepared in a glove box, on glass substrates, spun at 6000 rpm, where toluene was dropped onto the spinning film at approximately 5 sec. Substrates were then annealed at 70°C for $\sim 5 \text{ min}$. Film thickness was measured by a profilometer, where films prepared at 0.4 M and 0.32 M were $\sim 110 \pm 5 \text{ nm}$, and $\sim 90 \pm 5 \text{ nm}$. Lastly, films were coated with a thin film of polymethylmethacrylate (PMMA) dissolved in chlorobenzene to limit interaction of the film with water and oxygen from ambient air during ASE measurements.

RESULTS AND DISCUSSION

Films were prepared using an analogous protocol to a report on the fabrication of high performance MAPbI_3 based quasi 2D LEDs.¹² In this way, films used for ASE measurements are also potentially useful for electrically driven lasers. In the referenced work, films with a 20% excess of MA cation worked well for LEDs. Similarly, we used a 20% excess of MA beyond stoichiometric balance for a given order of PEA based quasi 2D perovskite. As the solutions were not stoichiometric, the order of perovskite was defined by the concentration of PEA in solution. Example perovskite LEDs were prepared to demonstrate that films were approximately device relevant (Fig. S2). Additionally, these films are reported to be very flat for moderate concentrations of bulky cation. This is consistent with our atomic force microscope images shown in Fig. 2, where the root mean square roughness decreased with increasing concentration of PEA cation (e.g. 3D $\sim 3.6 \text{ nm}$ roughness to 2.0 nm for $n=12$). ASE threshold was reported to be linearly proportional to film thickness,¹⁴ so thinner films are generally better for lasing applications due to better confinement. However, if the film is too thin, confinement is reduced due to evanescent losses. Films prepared at a given concentration had



approximately the same thickness regardless of order n . For example films at 0.4

Figure 2. Atomic force microscopy reveals that the addition of PEA cation can reduce surface roughness. Images show perovskite films (0.4 M solution) prepared on glass for a) 3D-MAPbI₃, b) PEA based quasi 2D perovskite $n=32$, and c) PEA based quasi 2D perovskite $n=12$

M were 110 \pm 5 nm for both 3D and order 12 films. Differences in thickness or roughness likely cannot explain differences in ASE threshold. This recipe was compatible with device fabrication and provided reasonably low ASE thresholds from 3D films.

Films prepared for ASE measurements were spun onto glass substrates and covered with a thin film of PMMA to limit the interaction between the film and air. These films were then

subjected to a pulsed nitrogen laser (337 nm) normal to the film surface and the resultant photoluminescence (PL) was measured from the film edge (insert Fig. 3a). Example spectra for a quasi 2D perovskite film ($n=12$) are shown in Fig. 3a. We see that the ASE peak emerges only when excited at intensities above the threshold, confirming that the peak originates from ASE and is not a resonance feature. Additionally, we performed a variable stripe length measurement for an example quasi 2D film ($n=32$, Fig. S3). From this data, we can estimate the gain and gain lifetime of this film to 110 cm^{-1} , and ~ 5 ps. The PL intensity is plotted as a function of pump fluence for a set of quasi 2D perovskite films from order 12, up to pure 3D (Fig. 3b). We can see that all films presented showed ASE behavior, characterized by a rapid rise in PL intensity. There are two things that are apparent from Fig. 3b. Quasi 2D perovskite generally increased in PL intensity with increasing order for a given pump fluence. Secondly, the ASE threshold decreased with increasing order. This is consistent with what we would expect based on existing reports for 2D and 3D perovskite.

To better understand the trend between ASE threshold and perovskite order, threshold is presented in terms of the molar concentration ratio of PEA to lead iodide in Fig. 3c. Perovskite films with an n value lower than order 12 did not always produce an ASE peak and are not presented here. It is possible that the ASE threshold is close to the damage threshold of the film. It should be noted that concentration is inversely proportional to the order n , which has been correlated to exciton binding energy.¹¹ In Fig. 3c we can see a linear trend, where the linear fit provides a line with an intercept 14 \pm 1 $\mu\text{J}/\text{cm}^2$, consistent with the ASE threshold measured for 3D films. The fit value was slightly higher than the current lowest measured value of 6 $\mu\text{J}/\text{cm}^2$ provided in literature for MAPbI₃.² The fit provides a slope of $\sim 220 \pm 10 \mu\text{J}/(\text{mols PEAI}/\text{mols PbI}_2)$. In the case of 2D perovskite there are 2 mols PEAI for every mol of PbI₂, we extrapolated an ASE threshold of $\sim 450 \pm 20 \mu\text{J}/\text{cm}^2$ for 2D perovskite, which is lower than the value predicted of 1.4 mJ/cm² by Chong et al,¹⁰ but may still be above the damage threshold of the film.

It is possible to further reduce the ASE threshold of quasi 2D films by reducing the thickness. In Fig. S4 we prepared 3D films at lower concentrations and found an approximate optimum concentration at 0.32 M, which provided a slightly lower threshold of $\sim 13 \mu\text{J}/\text{cm}^2$. Quasi 2D perovskite films at 0.32 M are presented in Fig 2c. At this concentration, we see that the minimum threshold was fixed at $\sim 14 \mu\text{J}/\text{cm}^2$, but allowed for higher concentrations of PEA before a threshold increase was observed. Quasi 2D films may benefit from the improved stability provided by the surface passivation effects of the PEA cation similar to reports for solar cells.²⁴ Passivation of surface traps by a quenching PCBM layer was previously shown to not change the ASE threshold.¹⁷ This is consistent with films prepared with low concentrations of PEA at 0.32 M, where the threshold was fixed at the pure 3D value despite the addition of passivating PEA. At this concentration, the threshold no longer linearly increased with the concentration of PEA. This suggests there is some property of the MAPbI₃ film that is limiting

threshold rather than PEAI. This is either intrinsic or a trap state that is relevant at fast time scales (~ 10 ps). Passivation of

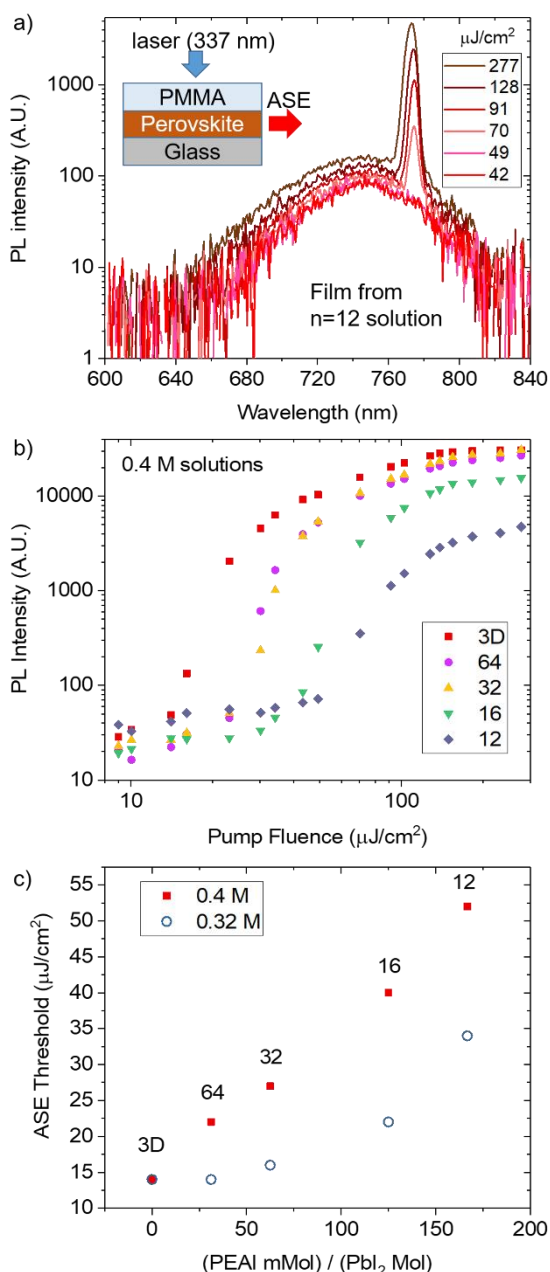


Figure 3. The photoluminescent intensity versus pump fluence of quasi 2D perovskite. a) Shows an example film of $n=12$ at different fluence. The insert shows a diagram of the experimental set-up. b) Log-log plot of the PL intensity of an example set of perovskite films as a function of order and pump intensity. As the order of quasi 2D perovskite increases, the PL intensity increases, while the threshold decreases. c) ASE threshold increases approximately linearly with concentration of PEAI at solution concentrations of 0.4 M. The threshold of quasi 2D films can be reduced further by reducing solution concentrations to 0.32 M.

surface defects should still be beneficial for light emitting diodes and electrically driven lasers. For a fixed deposition condition, we propose that in general a higher order films will likely still have lower thresholds.

Just like the broad spontaneous emission PL at low excitation energies, the ASE peak blue shifted with decreasing order. The wavelength of the spontaneous PL peak was correlated with a $1/n$ relation and the PEAI concentration.¹¹ A

similar trend was observed for the ASE peak location and is shown in Fig. S5. Additionally, the ASE peak location was found to shift with increasing pump fluence. At high pump fluence, the ASE peak broadened and blue shifted. This is shown for an example film of order 32 in Fig. 4a. These effects were attributed to Moss-Burstein shift, where conduction and valence bands fill with electrons and holes at high pump fluence, effectively increasing the band gap.¹⁸ At low pump fluence, there appears to be a slight red shift in the ASE peak. Similar red shifts are reported for experiments using 2 photon pumping of large perovskite crystals,²⁰ and experiments that focused deeper into perovskite crystals.²¹ Both works claimed red shifting was due to lower influence from surface states. For quasi 2D perovskite films, red shifting with fluence may be due to the filling of surface states followed by excitation of the bulk. The PL peak location and ASE peak location as a function of fluence is plotted for various orders of quasi 2D perovskite in Fig. 4b. We can see that the ASE peak location red shifted with increasing order. Within Fig. 4b the small red shift with fluence is only noticeable for higher order quasi 2D perovskite where thresholds were sufficiently low, and more difference existed between surface and bulk. For 3D perovskite, we observed a red shift when the film was not annealed, and less dependence of the ASE peak location on fluence. This indicates that annealing likely influences the formation of surface states.

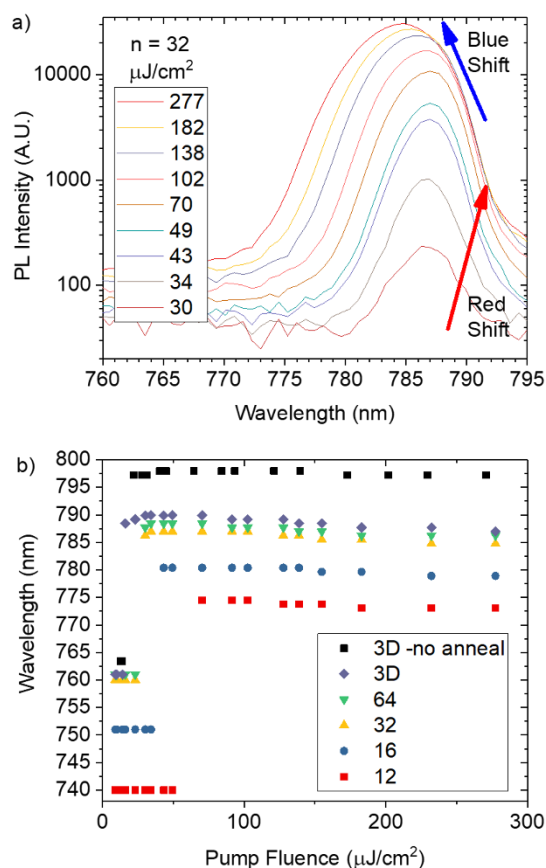


Figure 4. Peak location shifts with pump fluence. a) Shows an example quasi 2D perovskite film of order 32. We can see how the ASE peak location shifted with increasing fluence. The red shift was attributed to surface effects, while the blue shift and broadening were due to the Moss-Burstein effect. b) Shows that both

the maximum value of the spontaneous emission peak (bottom left) and ASE peak (top right) red shifted with increasing order.

Models for 3D perovskite suggest that radiative recombination at low frequency pumping is dominated by free carriers at low pump fluence, and spatially correlated pairs at high pump fluence.²¹ The ASE process is reported to quickly radiatively recombine within 10 picoseconds or shorter, but measurement times were limited by instrumentation.²² This value is consistent with our gain lifetime estimated by variable stripe length measurements. According to transient absorption spectroscopy, the inter-grain charge transfer process requires approximately 100 picoseconds to 1 nanosecond to complete.¹¹ This charge transfer rate appears to be one to two orders of magnitude slower than the radiative recombination rate of the ASE process. This suggests that inter-grain charge transfer should not significantly contribute to ASE. We measured the photoluminescent quantum yield (PLQY) using a steady state light source and found no direct correlation between PLQY and ASE threshold (Fig S6). The spontaneous emission process is enhanced by charge transfer and reduced by surface traps, while the ASE process is not, which obscures a correlation between ASE threshold and PLQY.

It seemed possible that excited state absorption could be limiting the performance of quasi 2D films. Perovskite is also known to have photo induced absorption (PIA), where the absorption coefficient is related to carrier concentration (N) and pump frequency (ω) ($\text{PIA} \propto N^{1/3}/(\omega^{1/2})$).²⁴ Although not directly discussed, this absorption appears to be in transient absorption spectra of quasi 2D perovskite.¹¹ This will become more pronounced at higher carrier concentrations ($\text{PIA} \propto N^{1/3}$) and should play some role in ASE behavior when pumped at 337 nm. However, there is no indication that this effect is more pronounced for quasi 2D perovskites than for 3D and likely cannot explain the increasing ASE threshold. The transient absorption spectra of low order ($n=1, 2, 3$) have 2 pronounced narrow band features, that appear as a neighboring increase and decrease in absorption. This effect is attributed to a blue shift from exciton resonance, and not bleaching, as the sum change in absorption is approximately zero.²⁵ This behavior should not affect the ASE threshold. We measured that the PL and absorption edge blue shifted in tandem with decreasing PEA concentration (Fig. S7), which indicated that the average order decreased. However, determining an accurate dimensionality distribution within a film is difficult. To further discuss what happens during the ASE process we made assumptions about the constituents of the quasi 2D film (Fig. S8). Varying distributions may broaden the PL from a film without charge transfer and affect the ASE threshold but cannot explain the ASE in films of single dimensionality (e.g. 2D).

It is possible that there exists a charge transfer state that is competing for excitons with ASE. This state needs to be at a similar energy level to the final emitter (e.g. 3D perovskite), as the transfer process is faster than spontaneous emission at room temperature. If this state were slightly below the energy level of an exciton in a given grain, it would be easy to enter the charge transfer state, but maybe comparatively slow to leave. In this way, it would compete for excitons, but not transfer fast

enough to contribute to ASE. It is natural to assume that the charge transfer state exists at the grain boundary, where charge would have to transfer from one grain to another. In quasi 2D perovskite the grain boundary is defined by PEA, and therefore it is reasonable that the amount of charge transfer is proportional to PEA. If the PEA charge transfer state is competing with ASE we would expect to see the linear increase

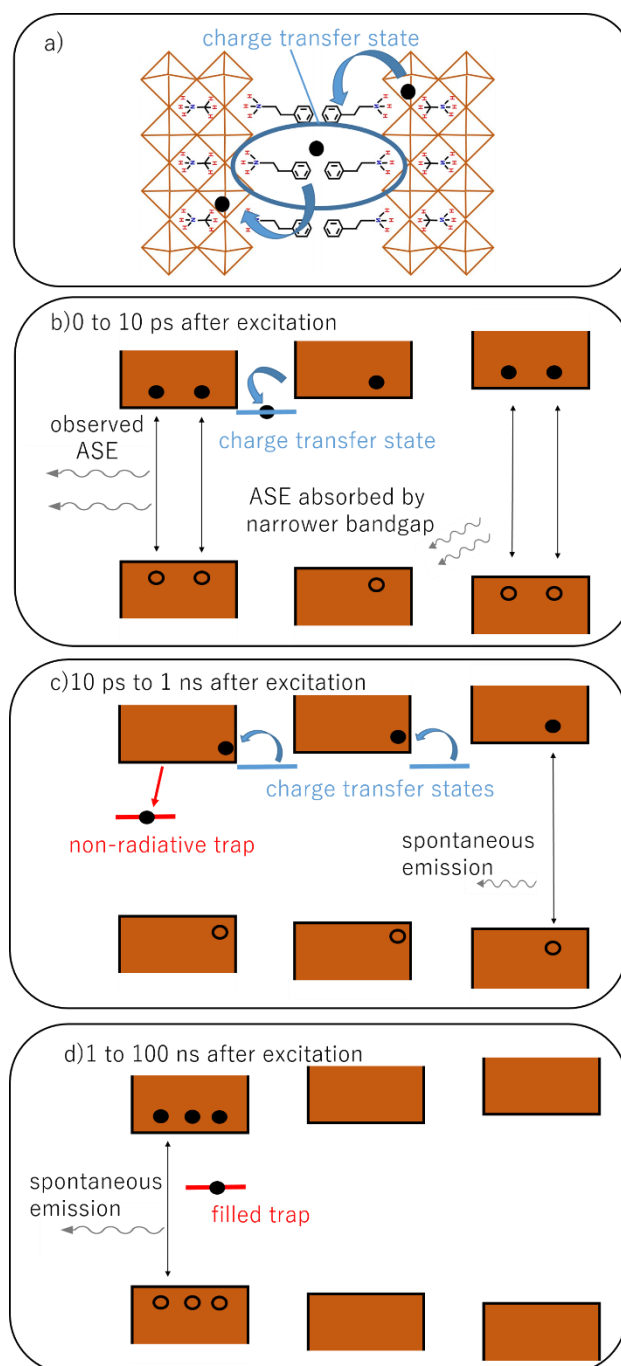


Figure 5. Proposed emission and charge transfer process in quasi 2D perovskite. a) Location of the charge transfer state is likely at the interface between two grains. b) At time scales up to 10 ps ASE will be the dominant process, however the charge transfer state will compete for excitons. High enough concentrations of the charge transfer state will prevent ASE. Any possible stimulated emission from higher order grains may be absorbed by lower orders, limiting ASE. c) At time scales from 10 ps to 1 ns ASE will largely be complete. Most excitons will have transferred, or be in the process of transfer. Transfer to non-radiative traps may limit spontaneous emission in higher orders. Low orders are well passivated and have higher rates of spontaneous emission. d) At 1 to 100 ns charges should be

completely transferred to the nearby highest order. The consolidation of charges allows for the filling of traps and relatively efficient spontaneous emission.

in threshold with concentration as seen in Fig. 2c. This state can also explain why the ASE threshold is so high in 2D perovskite, where there is no broadening from a distribution of orders. In 2D perovskite, this PEA boundary state would have to fill prior to ASE. As this explanation conceptually agrees with all orders regardless of assumed distribution, we believe that this is most likely the dominant mechanism explaining the linear ASE threshold increase with the concentration of PEA. A diagram of the proposed mechanism with approximate time scales is presented in Fig. 5. A charge transfer state is in contrast to the alternative, where charge tunnels across the double layer of PEA.

CONCLUSION

We showed that ASE is possible in PEA based quasi 2D perovskites and that the peak location shifted along with the broad band spontaneous emission peak as order decreased. The ASE threshold of quasi 2D perovskites increased approximately linearly with increasing concentration of PEAI at concentrations of 0.4 M. This linear increase was attributed to the existence of a charge transfer state at the PEA containing grain boundary. The charge transfer process is not fast enough to significantly contribute to ASE, but the charge transfer state will accept excitons and hinder ASE the threshold. A broadening distribution of PL approaching lower orders may also affect ASE threshold, but cannot explain the high threshold in low order single phase material. These results suggested that the low order quasi 2D perovskites used in LED applications are less suitable for lasing applications than higher order films or 3D counterparts. Films prepared at 0.32 M concentrations with average n values of 32 and above had little negative impact on ASE threshold from PEAI, but the presence of PEA may improve the performance and stability of LEDs and lasers.

Conflicts of interest

There are no conflicts to declare

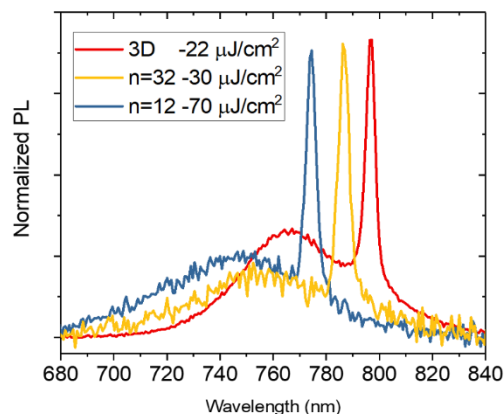
Acknowledgments

This work was supported by the Japan Science and Technology Agency (JST), ERATO, Adachi Molecular Exciton Engineering Project, under JST ERATO Grant Number JPMJER1305, Japan. We would like to thank Masayuki Yokoyama, Takeshi Komino and Fatima Bencheikh for helpful discussion.

References

- 1 S. A. Veldhuis, P. P. Boix, N. Yantara, M. Li, T. C. Sum, N. Mathews and S. G. Mhaisalkar, Perovskite Materials for Light-Emitting Diodes and Lasers, *Adv. Mater. Deerfield Beach Fla*, 2016, **28**, 6804–6834.
- 2 F. Yuan, Z. Wu, H. Dong, J. Xi, K. Xi, G. Divitini, B. Jiao, X. Hou, S. Wang and Q. Gong, High Stability and Ultralow Threshold Amplified Spontaneous Emission from Formamidinium Lead Halide Perovskite Films, *J. Phys. Chem. C*, 2017, **121**, 15318–15325.
- 3 F. Deschler, M. Price, S. Pathak, L. E. Klintberg, D.-D. Jarausch, R. Högler, S. Hüttner, T. Leijtens, S. D. Stranks, H. J. Snaith, M. Atatüre, R. T. Phillips and R. H. Friend, High Photoluminescence Efficiency and Optically Pumped Lasing in Solution-Processed Mixed Halide Perovskite Semiconductors, *J. Phys. Chem. Lett.*, 2014, **5**, 1421–1426.
- 4 M. Saliba, S. M. Wood, J. B. Patel, P. K. Nayak, J. Huang, J. A. Alexander-Webber, B. Wenger, S. D. Stranks, M. T. Hörlantner, J. T.-W. Wang, R. J. Nicholas, L. M. Herz, M. B. Johnston, S. M. Morris, H. J. Snaith and M. K. Riede, Structured Organic-Inorganic Perovskite toward a Distributed Feedback Laser, *Adv. Mater.*, 2016, **28**, 923–929.
- 5 H. Zhu, Y. Fu, F. Meng, X. Wu, Z. Gong, Q. Ding, M. V. Gustafsson, M. T. Trinh, S. Jin and X.-Y. Zhu, Lead halide perovskite nanowire lasers with low lasing thresholds and high quality factors, *Nat. Mater.*, 2015, **14**, 636.
- 6 A. S. D. Sandanayaka, T. Matsushima, F. Bencheikh, K. Yoshida, M. Inoue, T. Fujihara, K. Goushi, J.-C. Ribierre and C. Adachi, Toward continuous-wave operation of organic semiconductor lasers, *Sci. Adv.*, 2017, **3**, e1602570.
- 7 R. L. Milot, G. E. Eperon, T. Green, H. J. Snaith, M. B. Johnston and L. M. Herz, Radiative Monomolecular Recombination Boosts Amplified Spontaneous Emission in HC(NH₂)₂SnI₃ Perovskite Films, *J. Phys. Chem. Lett.*, 2016, **7**, 4178–4184.
- 8 M. Era, S. Morimoto, T. Tsutsui and S. Saito, Organic-inorganic heterostructure electroluminescent device using a layered perovskite semiconductor (C₆H₅C₂H₄NH₃)₂PbI₄, *Appl. Phys. Lett.*, 1994, **65**, 676–678.
- 9 T. Kondo, T. Azuma, T. Yuasa and R. Ito, Biexciton lasing in the layered perovskite-type material (C₆H₁₃NH₃)₂PbI₄, *Solid State Commun.*, 1998, **105**, 253–255.
- 10 W. Kiang Chong, K. Thirumal, D. Giovanni, T. Wee Goh, X. Liu, N. Mathews, S. Mhaisalkar and T. Chien Sum, Dominant factors limiting the optical gain in layered two-dimensional halide perovskite thin films, *Phys. Chem. Chem. Phys.*, 2016, **18**, 14701–14708.
- 11 M. Yuan, L. N. Quan, R. Comin, G. Walters, R. Sabatini, O. Voznyy, S. Hoogland, Y. Zhao, E. M. Beauregard, P. Kanjanaboos, Z. Lu, D. H. Kim and E. H. Sargent, Perovskite energy funnels for efficient light-emitting diodes, *Nat. Nanotechnol.*, 2016, **11**, 872.
- 12 Z. Xiao, R. A. Kerner, L. Zhao, N. L. Tran, K. M. Lee, T.-W. Koh, G. D. Scholes and B. P. Rand, Efficient perovskite light-emitting diodes featuring nanometre-sized crystallites, *Nat. Photonics*, 2017, **11**, 108.
- 13 N. Wang, L. Cheng, R. Ge, S. Zhang, Y. Miao, W. Zou, C. Yi, Y. Sun, Y. Cao, R. Yang, Y. Wei, Q. Guo, Y. Ke, M. Yu, Y. Jin, Y. Liu, Q. Ding, D. Di, L. Yang, G. Xing, H. Tian, C. Jin, F. Gao, R. H. Friend, J. Wang and W. Huang, Perovskite light-emitting diodes based on solution-processed self-organized multiple quantum wells, *Nat. Photonics*, 2016, **10**, 699.
- 14 R. Wang, Y. Tong, A. Manzi, K. Wang, Z. Fu, E. Kentzinger, J. Feldmann, A. S. Urban, P. Müller-Buschbaum and H. Frielinghaus, Preferential Orientation of Crystals Induced by Incorporation of Organic Ligands in Mixed-Dimensional Hybrid Perovskite Films, *Adv. Opt. Mater.*, n/a-n/a.
- 15 Li Meili, Gao Qinggang, Liu Peng, Liao Qing, Zhang Haihua, Yao Jiannian, Hu Wenping, Wu Yishi and Fu Hongbing, Amplified

- Spontaneous Emission Based on 2D Ruddlesden–Popper Perovskites, *Adv. Funct. Mater.*, 2018, **0**, 1707006.
- 16 T. Komino, H. Nomura, M. Yahiro, K. Endo and C. Adachi, Dependence of the Amplified Spontaneous Emission Threshold in Spirofluorene Thin Films on Molecular Orientation, *J. Phys. Chem. C*, 2011, **115**, 19890–19896.
- 17 L. N. Quan, M. Yuan, R. Comin, O. Voznyy, E. M. Beauregard, S. Hoogland, A. Buin, A. R. Kirmani, K. Zhao, A. Amassian, D. H. Kim and E. H. Sargent, Ligand-Stabilized Reduced-Dimensionality Perovskites, *J. Am. Chem. Soc.*, 2016, **138**, 2649–2655.
- 18 G. Xing, N. Mathews, S. S. Lim, N. Yantara, X. Liu, D. Sabba, M. Grätzel, S. Mhaisalkar and T. C. Sum, Low-temperature solution-processed wavelength-tunable perovskites for lasing, *Nat. Mater.*, 2014, **13**, 476.
- 19 J. S. Manser and P. V. Kamat, Band filling with free charge carriers in organometal halide perovskites, *Nat. Photonics*, 2014, **8**, 737.
- 20 Z.-Y. Zhang, H.-Y. Wang, Y.-X. Zhang, K.-J. Li, X.-P. Zhan, B.-R. Gao, Q.-D. Chen and H.-B. Sun, Size-dependent one-photon- and two-photon-pumped amplified spontaneous emission from organometal halide $\text{CH}_3\text{NH}_3\text{PbBr}_3$ perovskite cubic microcrystals, *Phys. Chem. Chem. Phys.*, 2017, **19**, 2217–2224.
- 21 T. Yamada, Y. Yamada, Y. Nakaike, A. Wakamiya and Y. Kanemitsu, Photon Emission and Reabsorption Processes in $\text{CH}_3\text{NH}_3\text{PbBr}_3$ Single Crystals Revealed by Time-Resolved Two-Photon-Excitation Photoluminescence Microscopy, *Phys. Rev. Appl.*, 2017, **7**, 014001.
- 22 L. H. Manger, M. B. Rowley, Y. Fu, A. K. Foote, M. T. Rea, S. L. Wood, S. Jin, J. C. Wright and R. H. Goldsmith, Global Analysis of Perovskite Photophysics Reveals Importance of Geminate Pathways, *J. Phys. Chem. C*, 2017, **121**, 1062–1071.
- 23 G. Xing, N. Mathews, S. S. Lim, N. Yantara, X. Liu, D. Sabba, M. Grätzel, S. Mhaisalkar and T. C. Sum, Low-temperature solution-processed wavelength-tunable perovskites for lasing, *Nat. Mater.*, 2014, **13**, 476–480.
- 24 Y. Yang, D. P. Ostrowski, R. M. France, K. Zhu, J. van de Lagemaat, J. M. Luther and M. C. Beard, Observation of a hot-phonon bottleneck in lead-iodide perovskites, *Nat. Photonics*, 2016, **10**, 53.
- 25 X. Wu, M. T. Trinh and X.-Y. Zhu, Excitonic Many-Body Interactions in Two-Dimensional Lead Iodide Perovskite Quantum Wells, *J. Phys. Chem. C*, 2015, **119**, 14714–14721.



TOC Image